Thermal and Morphological Study of a New Type of Nanocomposites: Functionalized PP / PA / Clay Nanocomposites

Hideko T. Oyama*, Yuko Oono**, and Kazuo Nakayama***

Research Center of Macromolecular Technology, National Institute of Advanced Industrial Science and Technology (AIST), 2-41-6 Aomi, Kohtoh-ku, Tokyo, 135-0064, Japan, *hideko-oyama@aist.go.jp, ** y-oono@aist.go.jp, *** kazuo-nakayama@aist.go.j

ABSTRACT

In the present work we explore a new type of nanocomposite, in which clay is distributed in a multi-phase polymer system. Our nanocomposites consist of an immiscible polymer pair, polypropylene grafted with maleic anhydride (PP-MAH) and polyamide 6 (PA), mixed with organo-modified synthetic mica. It was shown that (20/80/4) PP-MAH/PA/mica systems indicated that the mica was predominantly localized in the PA matrix in a composite prepared from PP-MAH with the lower MAH concentration. By contrast, in a composite prepared from PP-MAH with higher MAH concentration, the clay was located in both the PA and PP phases as well as at their interface. In this case, the PP dispersed phase, which was thermally unstable, was protected from thermal decomposition both by the wall of clay located at the interface and the dispersed clay in the PP phase. It was also found that copolymers formed *in situ* at the interface during melt-mixing also contributed to the thermal stability in a temperature range above 400 ^{o}C.

Keywords: nanocomposite, morphology, polypropylene, polyamide, clay

1 INTRODUCTION

The finding that nanoscale distribution of clay significantly improves polymer properties and extends their utility has stimulated extensive work in the field of polymer/clay nanocomposites in the last decade [1]. However, most studies thus far were carried out with simple single-phase polymer/clay systems. In the present study we explore new polymer/clay nanocomposites containing a multi-phase polymeric system.

2 EXPERIMENTAL

1.1 Materials

Table 1 lists the characteristics of PA and PP samples used in this study. Three types of PA with different molecular weights were obtained from Unitika, Japan, and two types of PP functionalized with different concentration of maleic anhydride (PP-MAH) were purchased from Aldrich Chemical Co. The organo-clay used in this study was a synthetic mica treated by dipolyoxyethylene alkyl(coco)methylammonium cation purchased from CO-OP Chemical, Japan, and its CEC was reported to be 120 meq/100g.

1.2 Melt-mixing

Materials were first dried under vacuum at 80 ^{o}C for 48 h prior to experiments. Melt-mixing was carried out in a HAAKE Minilab Rheomex with conical twin screws, which was operated at 240/260 ^{o}C at 50/100 rpm using a heating bath. The mixing time was fixed to be 10 min.

2.3 Analysis

Structure The obtained composites were cryotomed and

their morphology was examined by transmission electron microscopy (TEM). Two types of transmission electron microscopes were used for characterizing the samples. One was a Hitachi H-7000 TEM operated at an accelerating voltage of 75 kV for specimens stained by the vapor of ruthenium tetraoxide and the other was a LEO 922 energy-filtering TEM (EFTEM) operated at 200 kV for unstained specimens. Furthermore, light scattering measurements (LS) were carried out with an Otsuka Electronics Dyna 3000 in order to measure the mean particle size of the dispersed phase [2]. The composites were also characterized by wide-angle X-ray diffraction (WAXD), which was conducted using Cu K_α radiation (40kV, 300 mA) with an X-ray diffractometer (Rint 2500 VH/PC, Rigaku Co. Ltd.).

Properties A differential scanning calorimeter (Perkin Elmer DSC-7) was operated with a heating rate of 10 ^oC/min under a N_2 atmosphere. Dynamic thermal mechanical analysis (DMA) was carried out with Rheovibron DDV-25FP from Orientec Co. Ltd. at frequencies of 1, 3, 10, and 100 Hz at a heating rate of 2 ^oC/min between 150-250 ^oC. Moreover, thermogravi-metric analysis (TG) was performed using a Perkin Elmer Pyris 1 TGA at a heating rate of 10 ^oC/min under air atmosphere from room temperature to 800 ^oC.

3 RESULTS AND DISCUSSION

Figure 1 shows the WAXD profiles of organo-treated mica and two kinds of composites composed of (20/80/4) PP-MAH/M-PA/Mica with different MAH concentrations. The (001) peak originally observed for the mica disappears in both composites, which indicates that the clay does not have regular gallery space anymore in the composites.

Figure 2 and Figure 3 are EF-TEM micrographs of the composite prepared from PP-*l* MAH and from PP-*h* MAH, respectively. Figure 2 shows that the clay is predominantly localized in the PA matrix, whereas Figure 3 shows that it is located in both the PA and PP phases as well as at their interface. The LS data showed that the mean particle size of the dispersed phase decreases by addition of the clay, probably due to a contribution of enhanced melt viscosity of the PA matrix.

Next, the thermal stability of the composites in air was examined by TG. The results of a non-reactive blend of (20/80) i-PP/M-PA and the component polymers are shown in Figure 4. The comparison with the results of a reactive blend of (20/80) PP-*l* MAH/M-PA given in Figure 5 demonstrates that the reactive blend exceeds the non-reactive blend in thermal stability in a temperature range above 400 ^oC, which would be due to a contribution of copolymers formed *in situ* at the interface during melt-mixing. It is also shown that incorporation of clay significantly suppresses thermal decomposition of the PP dispersed phase in a temperature range between 300 and 400 ^oC. Figure 6 shows a difference in thermal stability between the composites prepared from PP-MAH with different MAH concentrations. It is clearly demonstrated that in a temperature range, in which the PP phase is decomposed, the composite prepared from PP-*h* MAH is much more stable compared to that prepared from PP-*l* MAH. This difference is probably caused by the difference in the clay distribution shown in Figures 2 and 3. The higher polarity of the PP-*h* MAH phase than the PP-*l* MAH phase would enable the clay to be located in both PA and PP phases as well as at the interface, which results in the effective protection of the PP dispersed phase from thermal decomposition.

Furthermore, DMA was measured in both composites, with the results given in Figure 7. A difference in dynamic storage modulus, *E'*, in the glassy state (*e.g.* –50 ^oC) and in the rubbery state (*e.g.* 120 ^oC) significantly decreases in the composites compared to neat PA. It is worth mentioning that the heat distortion temperature (HDT), which is located

between T_g and T_m, would significantly increase in the composites, especially in the composite prepared from PP-*h* MAH. The decrease in *E'* was negligible in this composite at T_g of PP, although it was not in the composite prepared from PP-*l* MAH. To shed further light on the situation DSC was undertaken in order to estimate the crystallinity, X_c, of the PP phase in both systems. The heat of fusion of PP was assumed to be 165 J/g [3], which resulted in X_c = 4.9 % in PP-*h* MAH/M-PA/Mica and 7.2 % in PP-*l* MAH/M-PA/Mica. This means that restriction of PP chain movements at T_g of PP in the former system is not due to crystallinity, but probably due to interactions with clay or crosslinkages formed in the dispersed phase. In conclusion, nanocomposites composed of multi-phase polymer system were observed to have unique stability properties in the present study.

REFERENCES

[1] A. Usuki, M. Kawasumi, Y. Kojima, Y. Fukushima, A. Okada, T. Kurauchi, and O. Kamigaito; *J. Mater. Res.,* **8**, 1179 (1993)

[2] K. Yamanaka, T. Inoue; Polymer 30, 662 (1989)

[3] J. E. Mark, Ed.; *Polymer Data Hand Book*, Oxford University Press: New York, Oxford (1999)

Table 1: Characteristics of materials.

	M_n (g/mol)*1	Functionality*1		T_m*2 (T_g*3)
		(wt%)	(#/chain)	(°C)
L-PA	14,000	0.44	1 COOH, 1 NH_2	219.5
M-PA	17,500	0.35	1 COOH, 1 NH_2	220.0 (62.7)
H-PA	21,500	0.28	1 COOH, 1 NH_2	219.0
PP-*l* MAH	10,000	0.6	0.6 MAH	163.2 (5.0)
PP-*h* MAH	3,900 M_w= 9,100	8~10	3.2~3.9 MAH	153.7 (--)

*1 reported values not analyzed values *2 DSC data *3 *E"* peak at 1 Hz measured by DMA

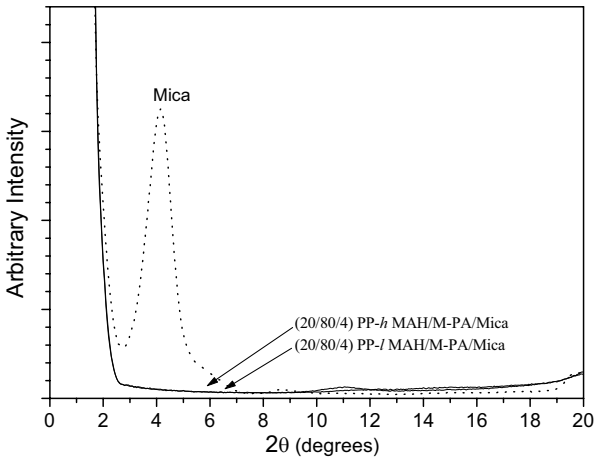

Figure 1: WAXD profiles of composites.

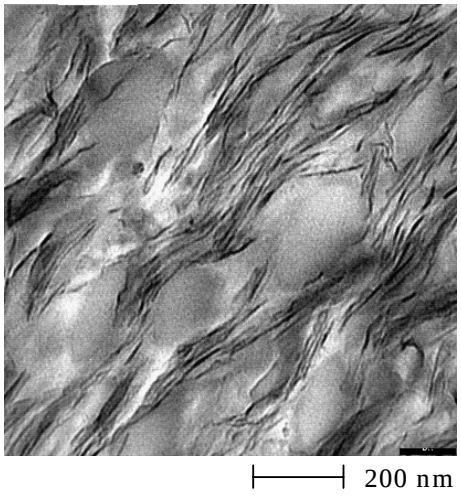

Figure 2: EFTEM micrograph of (20/80/4) PP-*l* MAH/M-PA/Mica.

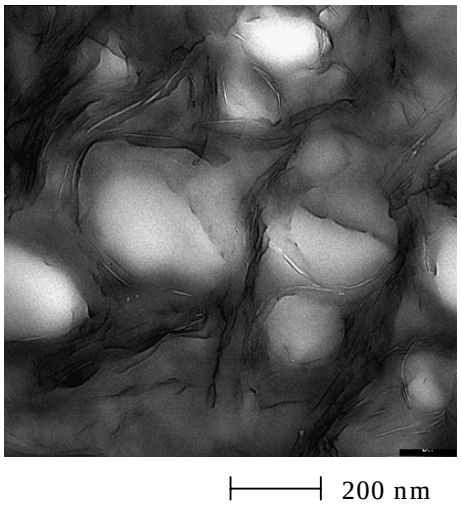

Figure 3: EFTEM micrograph of (20/80/4) PP-*h* MAH/M-PA/Mica.

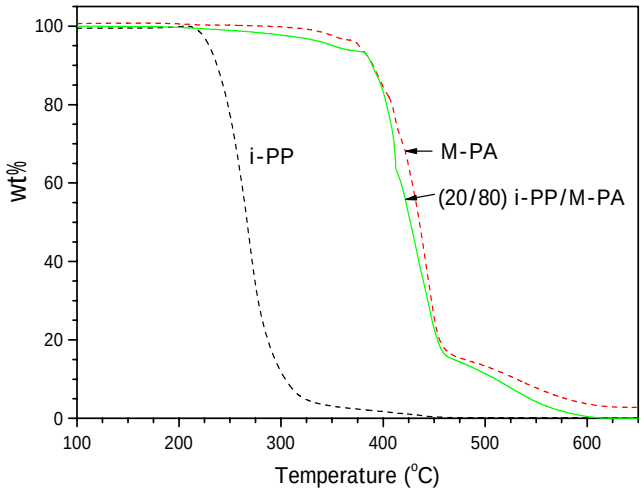

Figure 4: TG results of non-reactive blend composed of (20/80) i-PP/M-PA and the component polymers in air.

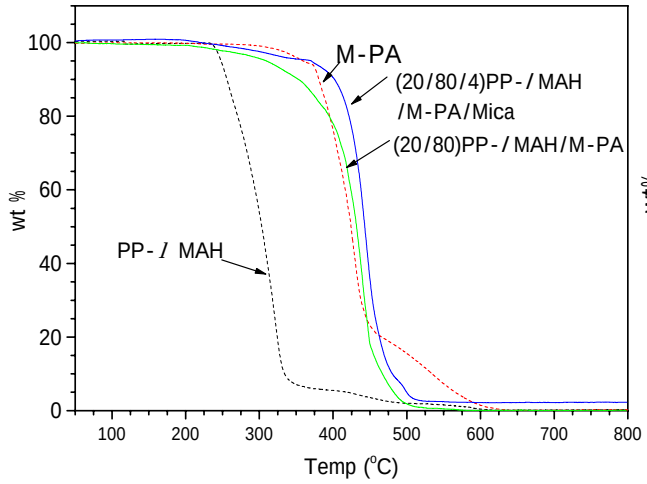

Figure 5: Effects of clay and copolymers formed *in situ* at the interface on thermal stability of composites in air.

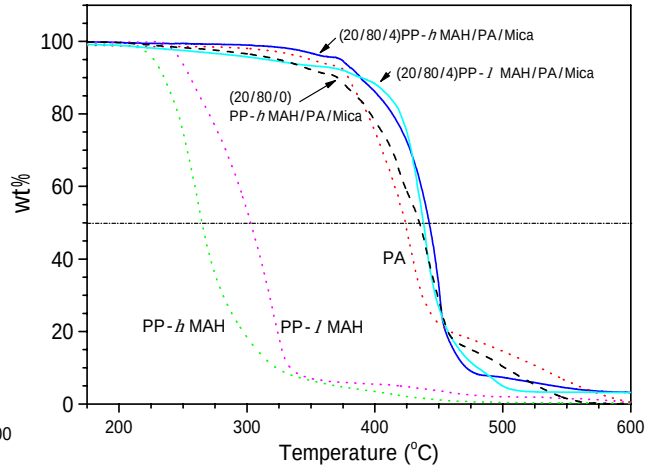

Figure 6: Effects of the MAH concentration incorporated to PP on thermal stability of composites in air.

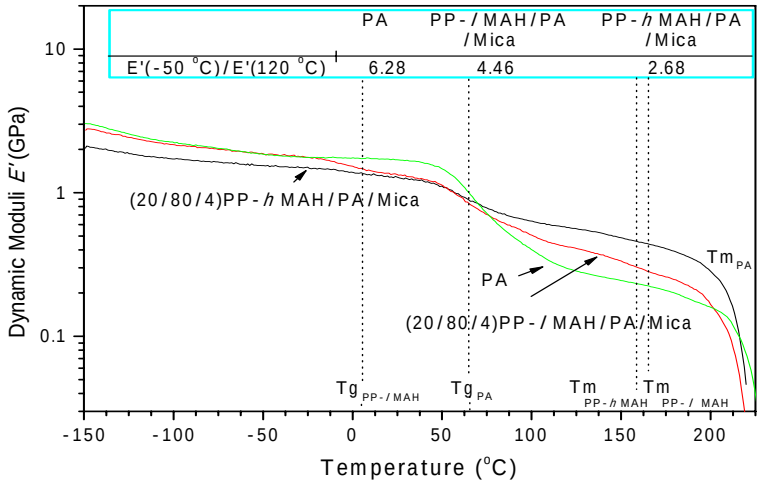

Figure 7: Dynamic storage modulus, *E'*, of the composites [DMA results measured at 1 Hz].